

Promising ferromagnetic Ni–Co–Al shape memory alloy system

K. Oikawa,^{a)} L. Wulff, and T. Iijima

National Institute of Advanced Industrial Science and Technology, Sendai 983-8551, Japan

F. Gejima, T. Ohmori, A. Fujita, K. Fukamichi, R. Kainuma, and K. Ishida

Department of Materials Science, Graduate School of Engineering, Tohoku University, Sendai 980-8579, Japan

(Received 5 March 2001; accepted for publication 4 September 2001)

A system of ferromagnetic β phase Ni–Co–Al alloys with an ordered $B2$ structure that exhibits the shape memory effect has been developed. The alloys of this system within the composition range Ni (30–45 at. %) Co–(27–32 at. %) Al, undergo a paramagnetic/ferromagnetic transition as well as a thermoelastic martensitic transformation from the β to the β' ($L1_0$) phase. The Curie and the martensitic start temperatures in the β phase can be controlled independently to fall within the range of 120–420 K. The specimens from some of the alloys undergoing martensitic transformation from ferromagnetic β phase to ferromagnetic β' phase are accompanied by the shape memory effect. These ferromagnetic shape memory alloys hold great promise as new smart materials. © 2001 American Institute of Physics. [DOI: 10.1063/1.1418259]

There is intense interest in the development of ferromagnetic shape memory alloys (FSMAs) as smart materials. In conventional SMAs, which are paramagnetic, the martensitic transformation underlying the shape memory effect is induced by means of changes in either temperature or stress or both. On the other hand, the same transformation in FSMAs can be triggered not only by changes in temperature and stress, but also by changes in the applied magnetic field. The response time of the shape changes accompanying magnetically controlled martensitic transformation are much faster than ones attendant on thermally controlled martensitic transformation. Compared with SMAs, therefore, it is expected that FSMAs would have wider applicability. To date, numerous FSMA candidate systems^{1–11} have been investigated including Ni₂MnGa,^{1–3} Ni₂MnAl,^{4–6} Fe–Pd,^{7,8} and Fe₃Pt¹¹ systems. Of these, the β phase of the most familiar alloy system, Ni₂MnGa, has a Heusler-type structure that undergoes martensitic transformation in the ferromagnetic state.¹ Both the conventional shape memory effect (SME) and the magnetic field-controlled SME (FSME) have been demonstrated in single crystals of Ni₂MnGa.^{1–3} Large displacements can be induced in these alloys by applied magnetic fields, giving rise to giant-magnetostriction values comparable or superior to the value associated with the well-known giant-magnetostrictive material Terfenol-D.¹ Ni₂MnAl,⁶ Fe–Pd,⁷ and Fe₃Pt¹¹ alloys also show similar magnetostriction. However, practical applications of these alloys are beset by several problems, such as extreme brittleness in the polycrystalline state and the high cost of constituent elements.

It is well known that the paramagnetic NiAl- β phase with $B2$ structure shows the SME.¹² Kainuma *et al.*¹³ investigated the effect of Co addition on the SME in the NiAl- β phase. They found that the β phase martensitically transformed into the β' phase ($L1_0$ structure) and that the martensitic transition temperature decreased with increased Co content. They also pointed out that the presence of a γ solid

solution [Al disordered face-centered-cubic (fcc) structure] as a second phase in the Ni–Co–Al system rendered the β phase ductile. The magnetic properties of the β phase in the Ni–Co–Al ternary system, however, were not clarified. In the present study, the magnetic and the shape memory properties of β -phase alloys in the Ni–Co–Al system have been investigated. A new group of FSMAs in the Ni–Co–Al β -based alloy system with high ductility at room temperature due to the presence of the γ solid solution phase has been identified.

Single β -phase and two-phase ($\beta + \gamma$) Ni–Co–Al alloys were prepared by melting electrolytic cobalt (99.9%), nickel (99.9%), and aluminum (99.7%) in an induction furnace under an argon atmosphere. After melting, each alloy was cast into a metal mold and the ingots obtained were hot rolled at 1573 K to a thickness of about 2 mm. Further cold rolling at room temperature was carried out to obtain samples of 150 μm thickness for bend tests. The β single-phase alloys exhibited very poor hot ductility, whereas the $\beta + \gamma$ two-phase alloys showed good hot fabricability and high room temperature ductility. Small pieces were cut from the ingots or from sheets and sealed in quartz capsules under argon atmosphere for heat treatment at various temperatures. The Curie temperature T_C and magnetization M were measured with a vibrating sample magnetometer, and the martensitic transformation temperature was measured by differential scanning calorimetry (DSC). The Curie temperature was taken as the minimum point in the plot of the temperature derivative of magnetization (dM/dT) vs temperature (T), at a field strength H of 500 Oe. This method of measuring T_C was adopted because no straight parallel lines of Arrot plots could be obtained. The method was previously adopted to yield reliable Curie temperatures.¹⁴ Quantitative measurement of the shape recovery associated with thermoelastic martensitic transformation was obtained by conventional bending tests at the martensitic transformation starting temperature M_s . Details of the bending test were described in our previous paper.¹³

^{a)}Electronic mail: k-oikawa@aist.go.jp

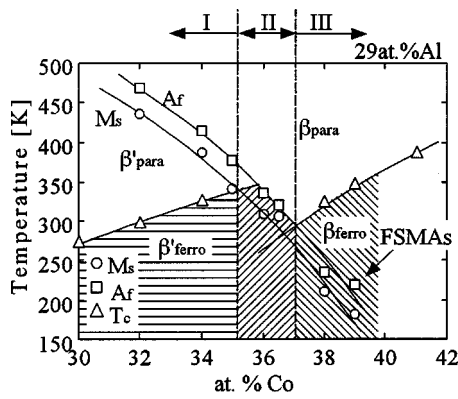


FIG. 1. Composition dependence of the Curie temperature T_C , the martensitic transformation temperature M_s and the austenitic finishing temperature A_f in $Ni_{71-x}Co_xAl_{29}$ alloys. The FSME can be observed in the hatched region.

Figure 1 shows the Curie temperature T_C , the martensitic transformation starting temperature M_s and the austenitic finishing temperature A_f as a function of the Co content in the 29 at. % Al section. T_C increases and M_s decreases with an increase in Co content, and the T_C and the M_s curves cross at around 35 at. % Co. The change in T_C with Co content implies that β -phase alloys in the Co-rich portion of the Co–Al binary system are ferromagnetic, with high T_C . It is very interesting to note that the extrapolated T_C for the martensite β' phase is about 85 K higher than that in the parent phase (β) at the same composition. In order to understand this unique behavior, combinations of magnetic transition and martensitic transformation are grouped into three types as shown in Fig. 1. Case I, paramagnetic β phase, martensitically transforms into paramagnetic β' , and eventually transforms into the ferromagnetic β' upon cooling. Case II, paramagnetic β phase, martensitically transforms into ferromagnetic β' upon cooling. Case III, paramagnetic β phase, transforms into ferromagnetic β phase, and then martensitically transforms into ferromagnetic β' phase upon cooling.

The T_C and M_s values for every β single-phase alloy are plotted in the Ni–Co–Al diagram, and estimated isocontour temperatures are given in Fig. 2. T_C increases with an increase in the Co content and a decrease in the Al content, while M_s decreases with an increase in both the Co and Al contents. The alloys in the hatched region in Fig. 2 fall into case II shown in Fig. 1. The values of T_C and M_s in these alloys can be individually controlled in the range of 120–420 K by changing the compositions of Co and Al. This temperature region is much wider than that for other FSMAs.^{1–11}

Figure 3 shows the magnetization versus temperature

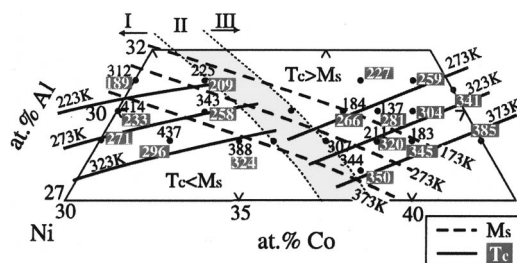


FIG. 2. Composition dependence of the Curie temperature T_C and the martensitic transformation temperature M_s in the Ni–Co–Al ternary system.

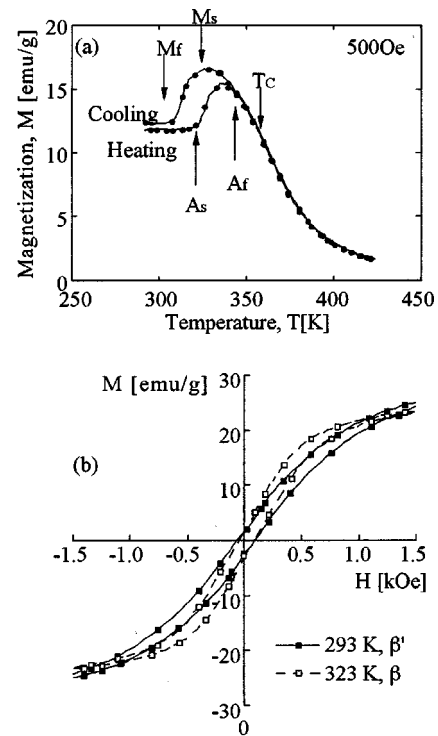


FIG. 3. Magnetic properties of the $Ni_{33.5}Co_{38.5}Al_{28}$ FSMAs. (a) $M-T$ curve in an external magnetic field of 500 Oe. (b) $M-H$ curves at 293 and 323 K upon heating. Note that the stable phase is β' at 293 K and β at 323 K.

($M-T$) curves at a field strength $H=500$ Oe and the magnetization versus external magnetic field ($M-H$) curves at several different temperatures for the $Ni_{33.5}Co_{38.5}Al_{28}$ β single-phase alloy, a typical FSMA in case III shown in Fig. 1. The heating and cooling magnetization curves show steps at M_s and A_s temperatures, respectively, as shown in Fig. 3(a). These steps in the $M-T$ curve at low magnetic field are observed in the Ni–Co–Al FSMAs because magnetization saturation is more easily accomplished in the β phase than in the β' phase as shown in Fig. 3(b). These results are similar to those seen in the case of Ni_2MnGa and Ni_2MnAl .^{1–6}

The plots shown in Fig. 4 are $M-T$ curves in different magnetic fields and $M-H$ curves at several temperatures for the $Ni_{35}Co_{35}Al_{30}$ β single-phase alloy falling within case II, whose M_s and A_s temperatures are located between the T_C of the parent β and the martensitic β' phases shown in Fig. 1. The magnetization value at a field strength of $H=500$ Oe sharply drops from 11 to 6 emu/g at 247 K upon heating and increases from 8 to 12 emu/g at 234 K upon cooling, as shown in Fig. 4(a). These step-like changes become smaller with an increase in the magnetic field. Figure 4(b) shows the hysteresis loops from 243 to 252 K at 3 K intervals. The magnetization value dramatically changes between 246 and 249 K. It should be noted that saturation magnetization is more easily achieved in the β' phase than in the β phase as shown in Fig. 4(b), contrary to the case shown in Fig. 3(b). This marked change in magnetization is caused by martensitic transformation from the paramagnetic parent phase to the ferromagnetic martensite phase. The T_C values for the β and β' phases of the $Ni_{35}Co_{35}Al_{30}$ alloy are estimated to be 217 and 263 K, respectively, by extrapolation. Because A_s of this alloy is higher than the T_C of β phase and lower than the T_C of β' phase, the β and β' phases are paramagnetic and ferromagnetic, respectively.

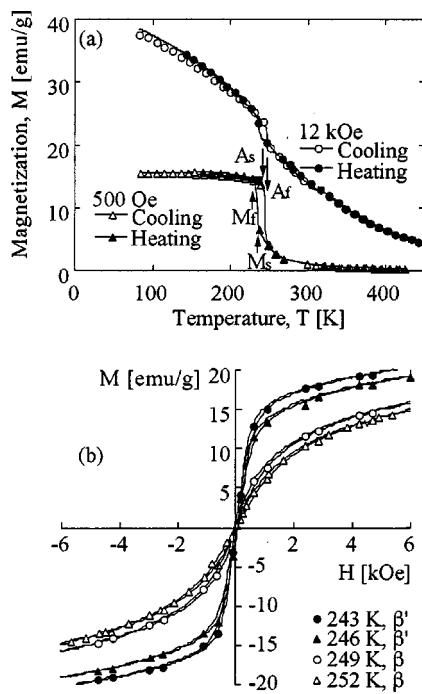


FIG. 4. Magnetic properties of the $\text{Ni}_{35}\text{Co}_{35}\text{Al}_{30}$ alloy. (a) M - T curves in external magnetic fields of 500 and 12 000 Oe. (b) M - H curves at 243, 246, 249, and 252 K upon heating. Note that the stable phase is β' at 243 and 246 K and β at 249 and 252 K.

romagnetic, respectively, at A_s . This explains why the magnetization of the M - H curve in the low magnetic field decreases at A_s as shown in Fig. 4.

The shape memory effect in the ferromagnetic state was examined by the bending test. Specimens of the two-phase ($\beta + \gamma$) alloy 150 μm thick, and $\text{Co}_{40}\text{Ni}_{33}\text{Al}_{27}$, with about 7 vol % γ , were heat treated at 1623 K for 2 min and at 1573 K for 15 min. The thin plates were bent to realize surface strain of 2% at M_s (260 K). Upon heating above A_f to 299 K, shape recovery of about 83% was obtained.

A key characteristic of FSMAs is large magnetic-field-induced strain. Recently, the change in length of a single crystal of a $\text{Ni}_{33}\text{Co}_{38}\text{Al}_{29}$ B2 alloy parallel to the applied magnetic field was measured by the three-terminal capacitance method. Large strain was confirmed. Details of the results will be reported in the near future.¹⁵

In conclusion, a FSMAs was found in the Ni-Co-Al β phase alloy system. This alloy system is characterized by good ductility and a wide range of transition temperatures compared with other FSMAs. The Curie temperature T_C of the β' phase is higher than that of the β phase, and this may lead to the design of sensors. For example, if stress is applied to the paramagnetic β phase alloys of case II at temperatures just above M_s , ferromagnetic β' phase would be induced. This means that changes in magnetization could be used to detect strain in a deformed material.

The authors wish to thank Dr. L. Chandrasekaran of the Structural and Materials Center, QinetiQ, Farnborough, UK, for useful comments and for help in the presentation of the manuscript for publication. A part of the present study was supported by a Grant-in-Aid for Scientific Research of the Ministry of Education, Science, Sports and Culture, Japan.

- ¹K. Ullakko, J. K. Huang, C. Kanter, V. V. Kokorin, and R. C. O'Handley, *Appl. Phys. Lett.* **69**, 1966 (1996).
- ²S. J. Murray, M. Marioni, A. Kukla, J. Robinson, R. C. O'Handley, and S. M. Allen, *J. Appl. Phys.* **87**, 5774 (2000).
- ³S. J. Murray, M. Marioni, S. M. Allen, and R. C. O'Handley, *Appl. Phys. Lett.* **77**, 886 (2000).
- ⁴F. Gejima, Y. Sutou, R. Kainuma, and K. Ishida, *Metall. Mater. Trans. A* **30A**, 2721 (1999).
- ⁵R. Kainuma, F. Gejima, Y. Sutou, I. Ohnuma, and K. Ishida, *Mater. Trans., JIM* **41**, 943 (2000).
- ⁶A. Fujita, K. Fukamichi, F. Gejima, R. Kainuma, and K. Ishida, *Appl. Phys. Lett.* **77**, 3054 (2000).
- ⁷R. D. James and M. Wuttig, *Philos. Mag. A* **77**, 1273 (1998).
- ⁸Y. Furuya, N. W. Hagoood, H. Kimura, and T. Watanabe, *Mater. Trans., JIM* **39**, 1248 (1998).
- ⁹O. Song, C. A. Balletine, and R. C. O'Handley, *Appl. Phys. Lett.* **64**, 2593 (1994).
- ¹⁰R. Hayashi, S. J. Murray, M. Marioni, S. M. Allen, and R. C. O'Handley, *Sens. Actuators A* **81**, 219 (2000).
- ¹¹T. Kakeshita, T. Takeuchi, T. Fukuda, T. Saburi, R. Oshima, S. Muto, and K. Kishio, *Mater. Trans., JIM* **41**, 882 (2000).
- ¹²K. Enami and S. Nenno, *Metall. Trans.* **2**, 1487 (1971).
- ¹³R. Kainuma, M. Ise, C. C. Jia, H. Ohtani, and K. Ishida, *Intermetallics* **4**, S151 (1996).
- ¹⁴H. Saito, T. Yokoyama, K. Fukamichi, K. Kamishima, and T. Goto, *Phys. Rev. B* **59**, 8725 (1999).
- ¹⁵A. Fujita, K. Fukamichi, K. Oikawa, F. Gejima, R. Kainuma, and K. Ishida (unpublished).